Vascular Pharmacology 120 (2019) 106568

Contents lists available at ScienceDirect

Vascular Pharmacology

journal homepage: www.elsevier.com/locate/vph

Stox1 induced the proliferation and cell cycle arrest in pulmonary artery smooth muscle cells via AKT signaling pathway

Yi Xu[a,b], Zengxian Sun[a,b], Qian Wang[c], Tianyan Wang[b], Yun Liu[b,*], Feng Yu[a,*]

[a] School of Basic Medicine and Clinical Pharmacy, China Pharmaceutical University, No.24,Tong Jia Xiang, Nanjing 210009, PR China
[b] Department of Pharmacy, The First People's Hospital of Lianyungang, No.182,TongguanNorth Road, Lianyungang 222002, PR China
[c] Anesthesiology Department, Children's Hospital of Soochow University, Suzhou 215025, China

ARTICLE INFO

Keywords:
Hypoxia
Pulmonary artery hypertension
Stox1
Proliferation

ABSTRACT

Background: Pulmonary arterial hypertension (PAH) is a life-threatening disease characterized by the vascular remodeling that also involves proliferation and migration of pulmonary artery smooth muscle cells (PASMCs). Overexpression of Storkhead box (STOX1) regulates genes involved hypoxia, redox balance, nitric oxide, and energy metabolism. In this study, we supposed Stox1 adjusted cells proliferation and migration in PASMCs development and played an important role in the pulmonary arterial vascular remodeling.

Methods: Hemodynamic assay and Right ventricular morphometric assay were used to check the rat model of PAH. HE staining was used to examine the arterial wall thickness. Masson staining showed that the deposition of collagen was significantly increased in PAH. In addition, Stox1 were assessed by immunofluorescence and immunohistochemistry staining. The effect of Stox1 on PASMCs was assessed by cell counting Kit-8 assay (CCK-8 assay), Scratch-Wound assay, EdU staining assay, Cell cycle analysis and Western blot.

Results: Right ventricular systolic pressure (RVSP) and right ventricular were significantly increased in hypoxia group and monocrotaline group compared to control group. The expression of Stox1 was increased in lung tissues in PAH rats. In vitro, the expression of Stox1 was up-regulated with time-dependent manner in hypoxia condition. Meanwhile, Stxo1 promoted the proliferation and migration in hypoxia-treated PASMCs. Moreover, we found that hypoxia promoted the expression of PCNA, Cyclin E and Cyclin A, increased more cells from G_0/G_1 phase to S phase and induced the activation of AKT proteins, which was significantly attenuated by inhibition of Stox1 expression in PASMCs.

Conclusion: These findings indicated that Stox1 induced proliferation of PASMCs and the effect is, at least in part, mediated through AKT signaling pathway.

1. Introduction

Pulmonary arterial hypertension (PAH) is a complex and intractable pulmonary vascular disease, characterized by an increase in pulmonary vascular remodeling, which is leading to right heart failure and eventually death [1]. Pulmonary arterial remodeling is a central process in the PAH pathogenesis by thickening of all layers of vascular walls [2,3]. Pulmonary arterial smooth muscle cell (PASMC), which is a kind of highly specialized and differentiated cell, is critical to the pathogenesis of pulmonary arterial remodeling [4,5]. Therefore, it is irreplaceable for the prevention and treatment of PAH that exploring the molecular mechanisms is responsible for PASMCs proliferation.

Storkhead box (STOX) protein 1, a winged-helix transcription factor structurally and functionally related to the fork-head family of transcription factors, plays a crucial role in regulating multiple biological processes in the expression of genes [6,7]. STOX1 overexpression regulated genes including the response to hypoxia, redox balance, nitric oxide, and energy metabolism [8,9]. Furthermore, STOX1 was found to promote mitotic entry and the proliferation of inner ear epithelial cells [10,11]. In addition, recently study reported that STOX1 had a pivotal role in cerebellar granule neurogenesis and medulloblastoma suppression [12]. Moreover, STOX1 induced phosphorylation of the longest human tau isoform at phosphor-epitopes typically found in neurofibrillary tangles in Alzheimer's disease [13,14].

The reason why we focused on Stox1 function in PAH was that, we found that TCONS_00034812 (a lncRNA located on chromosome 12 in the rats) could increase the Stox1 expression in PASMCs [15]. Further studies revealed that TCONS_00034812 and Stox1 could regulate PASMCs function through MAPK pathway. However, until recently, there is lack of knowledge on the role of Stox1 in pulmonary arterial

* Corresponding authors.
E-mail addresses: yunliu211315@163.com (Y. Liu), yufeng090130@163.com (F. Yu).

https://doi.org/10.1016/j.vph.2019.106568
Received 12 February 2019; Received in revised form 11 June 2019
Available online 14 June 2019

remodeling of PAH. According to our studies, we supposed Stox1 adjusted cells proliferation and migration in PASMCs development and played an important role in the pulmonary arterial remodeling.

The hope is that the question will be solved with our acquainted methods. Firstly, we indicated the expression of Stox1 in lung tissues from female rats in different conditions. Then we explored its roles on cell proliferation and migration in PASMCs by gene silencing approaches. In addition, flow cytometry assay and western blot assay were used to provide the mediation function of Stox1 on the cell cycle influence and AKT signaling pathways. Collectively, our study showed that the proliferation and cell cycle arrest of PASMCs induced by Stox1 were through the AKT signaling pathway.

2. Materials and methods

2.1. Reagents and antibodies

The antibodies against Stox1(Cat.No.14790–1-AP;1:1000), PCNA(Cat.No.10205–2-AP; 1:1000), Cyclin A (Cat.No.13295–1-AP;1:2000), Cyclin E (Cat.No.11554–1-AP;1:2000), AKT(Cat.No.10176–2-AP; 1:2000),and β-actin(Cat.No.60008–1-lg; 1:5000) were purchased from Protein TechGroup, Inc. (Chicago, IL, USA). The antibody against p-AKT (Cat.No.#9271; 1:1000) was from Cell Signaling Technology lnc. Monocrotaline (Cas#:315–22-0) was from Vicmed Biotech Co., Ltd. Cycle TEST™ PLUS DNA Reagent kit was obtained from BD Biosciences (FranklinLakes, NJ, USA). Enhanced chemiluminesence (ECL) kit and PBS were purchased from Nanjing Key Gen Biotech Co., Ltd. (Nanjing, China). Other reagents were purchased from common commercial sources.

2.2. Animal and rat lungs tissues

A total of 18 adult female rats (6–8 weeks old, weighting 200 g) were purchased from the Experimental Animal Center of Xuzhou Medical University (Grade II), China. The animal experimental protocols were approved by the Institutional Animal Care and Use Committee (IACUC). Adult rats were randomly separated into control group ($n = 6$), hypoxia group ($n = 6$) and monocrotaline group ($n = 6$) for 21 days [16]. Control group rats were fed in normoxia condition. Hypoxia group rats were fed in (3% O_2) hypoxia condition. Monocrotaline group rats were injected with 60 mg/kg monocrotaline once each rat [17]. All of the rats were fed with 60% relative humidity environment. At the end of 21 days exposure period, the rats were anesthetized using 35 mg/kg pentobarbital and excised the heart and lungs. The lung tissues were washed with cold PBS and fixed with pins in a dissection dish to isolate the pulmonary arteries in the arteries-up position under astereo-microscope. The lung tissues were stored at −80 °C for further studies.

2.3. Hemodynamic assay

The rats were anesthetized using 35 mg/kg pentobarbital. A 2–3 cm incision was made in the anterior cervical region. The subcutaneous tissue of the neck was obtusely separated and the external and internal jugular veins were carefully dissected avoiding bleeding and affecting the visual field. Then, a v-shaped incision was cut in external jugular or jugular vein. Miniature conduit connections pressure sensor (TSD104A pressure transducer, the BIOPAC Systems) filling with heparin saline solution (125 U/ml) was slowly inserted into the vein incision in the rat superior vena cava. According to waveform change from 16 channel of physiological signal recording analysis instrument, the miniature guide tube was gently and carefully advanced the catheter. The pipe was introduced into the right atrium, right heart and pulmonary artery. After close observation, the right ventricular systolic pressure (RVSP) was calculated.

2.4. Right ventricular morphometric assay

After hemodynamic assay, the anesthesia rats were cut the abdomen, then, carefully separated abdominal aorta, opened the chest cavity and cut off the trachea, superior vena cava and other connective tissues through the upper mediastinum. Next, the heart and lung were separated and put into PBS. Right ventricle was injected PBS solution at a slow and constant rate to lavage the heart and lung tissue. After that, right ventricle (RV) and left ventricle + ventricular septum (LV + S) were separated and weighed to calculate RV/ (LV + S).

2.5. Cell culture

Primary PASMCs were isolated from the pulmonary arteries vessels of the rats [18]. The pulmonary artery vessels was isolated out and washed with PBS to remove excess blood. Then the artery vessels were scraped of both the internal and external sides of the vessel wall to remove endothelial and fibroblast cells. The tissue was then rinsed several times with DMEM/F12 supplemented with 1% penicillin and streptomycin. Then, the tissue was minced into a tube with 2 mg/ml collagenase at 37 °C for 2 h. After concentrating 2000 g for 5 min, the supernatant was discarded and the sediment was mixed into a flask by complete culture (DMEM/F12 supplemented with 10% FBS and 1% penicillin/streptomycin) at 37 °C, 5% CO_2 incubator. Passages 3–6 and 60–90% confluence were used for further studies. When cells reached 90% confluence, they were digested with 0.25% trypsin and 0.01% EDTA for approximately 1 min at 37 °C 5% CO_2 culture incubator and passaged at a ratio of 1:2 or 1:3. PASMCs in hypoxia condition were incubated with a gas mixture containing 92% N_2, 5% CO_2 and 3% O_2. PASMCs were starved for 24 h in DMEM without serum before each experiment. Then cells were treated with different reagents as described in the results.

2.6. Cell transfection

To silence the expression of transcription factor Stox1, small interfering RNA (siRNA) were transfected into PASMCs which were designed and synthesized by Gene Pharma using HieffTrans™ Liposomal Transfection Reagent. The sequences of Stox1-rat-371 were as follows: sense 5'-GCUGUGUUAUAGCCCAUAUTT-3′ and antisenses: 5'-AUAUC GGCUAUAACACAGCTT-3′. The sequences of Stox1-rat-747 were as follows: sence 5'-GCAUGGCUCUAAGGACCUATT-3′ and antisense 5'-UAGGUCCUUAGAGCCAUGCTT-3′. The sequences of Stox1-rat-1194 were as follows: sense 5'-GCUGUGUUAUAGCCGAUAUTT-3′ and antisense 5'-AUAUCGGCUAUAACACAGCTT-3′. Nonsilencing siRNA (NC): sense 5'-UUCUCCGAACGUGUCACGUTT-3′ and antisense 5'-ACGUGA CACGUUCGGAGAATT-3′.

Liposomal Transfection Reagent (5 μl) from HieffTrans™ and small interfering RNA of Stox1 (5 μl) was diluted into 50 μl of serum-free DMEM medium respectively, and the two solutions were mixed and allowed to stand for 15 min at room-temperature. Then the mixture solution were added into the cell by incubating at 37 °C with 5% CO_2 for 6 h. Control and NC group cells were prepared in the same way using transfection reagent alone (mock) and NC. After 6 h incubation, the transfection medium was replaced by DMEM containing 3% FBS for 24 h. Then the PASMCs were incubated in different condition for 48 h.

2.7. Hematoxylin and eosin staining and masson trichrome staining

The lung tissues were sliced and immersed in 4% paraformaldehyde (PFA) overnight at room temperature in tissue blocks [19]. Then the slices were dehydrated with ethanol, butyl alcohol and cleared with PBS. After the slices were embedded in paraffin wax, the slices were cut into 5 μm thick longitudinal sections. The lung tissue sections follow were stained with hematoxylin and eosin or masson respectively.

2.8. Immunohistochemistry

As mentioned above, 5 μm paraffin-embedded lung tissue sections were deparaffinized and rehydrated in graduated alcohol [20]. Antibody was incubated with Stox1 (Cat.No.14790–1-AP;1:200) or β-actin (Cat.No.60008–1-lg; 1:200). Brown and yellow colors indicated positive stains. The sections were viewed with an Eclipse 600 Nikon microscope and photographed with a digital camera.

2.9. Cell proliferation assay

Cells were grown in 96-well plates and starved in DMEM without serum for 24 h. After treatment according to the experimental requirement, the supernatant was removed, then added 10 μl/well cell proliferation reagent WST-1 within 90 μl medium and shaken thoroughly for 1 min on a shaker. The absorbance was measured at a wavelength of 490 nm in a spectrophotometer.

2.10. Scratch-wound assay

PASMCs were cultured in 6-well plates. After the cells were drawn a line by 100 μl pipette tips, creating 1-mm-wide lane per well, and the detached cells were washed out by cold PBS. Then the cells were transfected with NC or siStox1 under normoxia or hypoxia conditions. Wounded areas were photographed at zero time. After 48 h of incubation, photographs were taken from the same areas as those recorded at zero time.

2.11. 5-Ethynyl-2′-deoxyuridine (EdU) staining

Cell proliferation was analyzed using kFluor647 Click-iTEdU kit (Nanjing KeyGen Biotech Co., Ltd.) according to the manufacturer's protocol [21]. PASMCs were seeded into 24-well cell culture plates at a density of 1×10^4 cells per well. Following transfection and treatment, the PASMCs were incubated with 10 μmol/l EdU for 4 h. Cells were permeabilized for 20 min with 0.5% Triton X-100 after fixing with 4% formaldehyde for 30 min at room temperature. Cells in each well were washed three times with 0.1 ml 3% bovine serum albumin (Cat. No. VIC018; Xuzhou VICMED Biological Technology Co., Ltd.) and subsequently incubated with 1× Click-iTEdU reaction buffer at room temperature for 30 min in the dark. The PASMCs nuclei stained by Hoechst were used to count cells and the visualization was performed using a fluorescence microscope (Nikon Corporation, Tokyo, Japan).

2.12. Flow cytometry

The transfected PASMCs were cultured in 60 mm plates [22]. To perform cell cycle analysis, the cells were digested with trypsin and fixed with 70% ethanol for 24 h at 4 °C. The cells were stained according to the manufacturer's protocol of CycleTEST PLUS DNA Reagent kit (BD Biosciences). The fixed cells were washed 3 times with PBS and centrifuged at 2000*g* for 5 min in room temperature. The supernatant was subsequently discarded. Cells were incubated with propidium iodide (PI) stain buffer for 10 min and subsequently treated with 200 μl of PBS, 200 μl of RNase A and 200 μl of PI for 10 min at 4 °C in the dark. Finally, the cells were screened by 400-mesh sieves and analyzed by flow cytometry (FACSCanto II; BD Biosciences). The results obtained were analyzed using the ModFit software (version 4.1; Verity Software House, Inc., Topsham, ME, USA).

2.13. Immunofluorescence

For immunofluorescence staining, PASMCs were fixed in 4% PFA for 30 min at room temperature, rinsed three times with cold PBS and permeabilized in 0.4% triton-X 100 for 5 min. After washing with PBS three times, the cells were blocked in 1% BSA for 30 min and incubated overnight at 4 °C with Stox1 antibody with 1:200 dilutions in 1% BSA. After extensive washes with PBS for 30 min, the cells were incubated with the secondary antibody IgG conjugated with rhodamine at a 1:500 dilution for 1 h at room temperature. DAPI (4, 6-diamidino-2-phenylindole) was used as mounting solution to label the nuclei, and the cells were observed for fluorescence images under a fluorescence microscope (Nikon Corporation, Tokyo, Japan).

2.14. Western blotting

PASMCs, after transfection with or without siStox1, were incubated in normal or hypoxia environments for 48 h respectively. Then, RIPA buffer (Santa Cruz) was used to lyse the cells for 30 min on ice. By centrifugation of the lysis at 13,500*g* for 15 min, the cell lysate supernatant were extracted as total protein to measure the concentrations of proteins by BCA kit from Beyotime Institute of Biotechnology (Haimen, China). Subsequently, Total protein (20 μg) from each sample was analyzed using 6–12% SDS-PAGE and then the gel was transferred onto polyvinylidenedifluoride (PVDF) membranes. After blocking with 5% non-fat milk in TBS-T for 1 h at 37 °C, The PVDF membranes were incubated with antibodies overnight at 37°C and washed 6 times with TBS-T at room temperature (5 min/wash). The PVDF membranes were shaken and incubated at room temperature for 1 h with horseradish peroxidase labeled secondary antibody. The secondary antibodies were goat-anti-rabbit immunoglobulin G (IgG) (cat. no. VA002; 1:5000; Xuzhou VICMED Biological Technology Co., Ltd., Xuzhou, China; www.vicmed.cn) and goat-anti-mouse IgG (cat. no. VA001; 1:5000; Xuzhou VICMED Biological Technology Co., Ltd.). Following 1 h incubating and 6 times (5 min/wash) thoroughly washing with TBS-T, the membranes were incubated with ECL solution for 5 min. Protein bands were visualized via VersaDoc™ MP 4000 (Bio-RadLaboratories, Inc.) and analyzed by using PDQuest Advanced 2D analysis software (version 8.0, Bio-Rad Laboratories, Inc.).

2.15. Statistical analysis

Data are expressed as the mean ± standard error of the mean. Comparisons between two groups were performed using unpaired Student's *t*-test and three or more groups were compared using one-way ANOVA, followed by Dunnett's test. Differences were considered to be significant at $P < .05$. analysis of data was made by GraphPad Prism program (San Diego, California, USA).

3. Result

3.1. RV hemodynamics and morphometry analysis in different group rats

In order to assess PAH model in rats, the Fulton index (the ratio of the weights of the free wall of the right ventricle to the weight RV/(LV + S) and RVSP measured and analyzed. Monocrotaline injection led to increase of RV/ (LV + S) ratio, while, hypoxia condition significantly increased RV/(LV + S) ratio twice times(Fig. 1A,B). Compared to control group, monocrotalien injection induced RVSP an elevation (Fig. 1C, D, E).The above results confirmed our models were establishment successfully.

3.2. Morphometric analysis of pulmonary vascular remodeling in lung tissues from the rats

To explore the Stox1 function on pulmonary arterial vascular remodeling in PAH, the morphology of pulmonary vessels were examined to show potential correlations of the morphological changes by hematoxylin-eosin stain (Fig. 2A, C). The wall thickness of the pulmonary artery in hypoxia group was twice compared with control group (Fig. 2B). Meanwhile, similar result was show in Fig. 2D, the monocrotaline group was over twice higher than control group at the wall

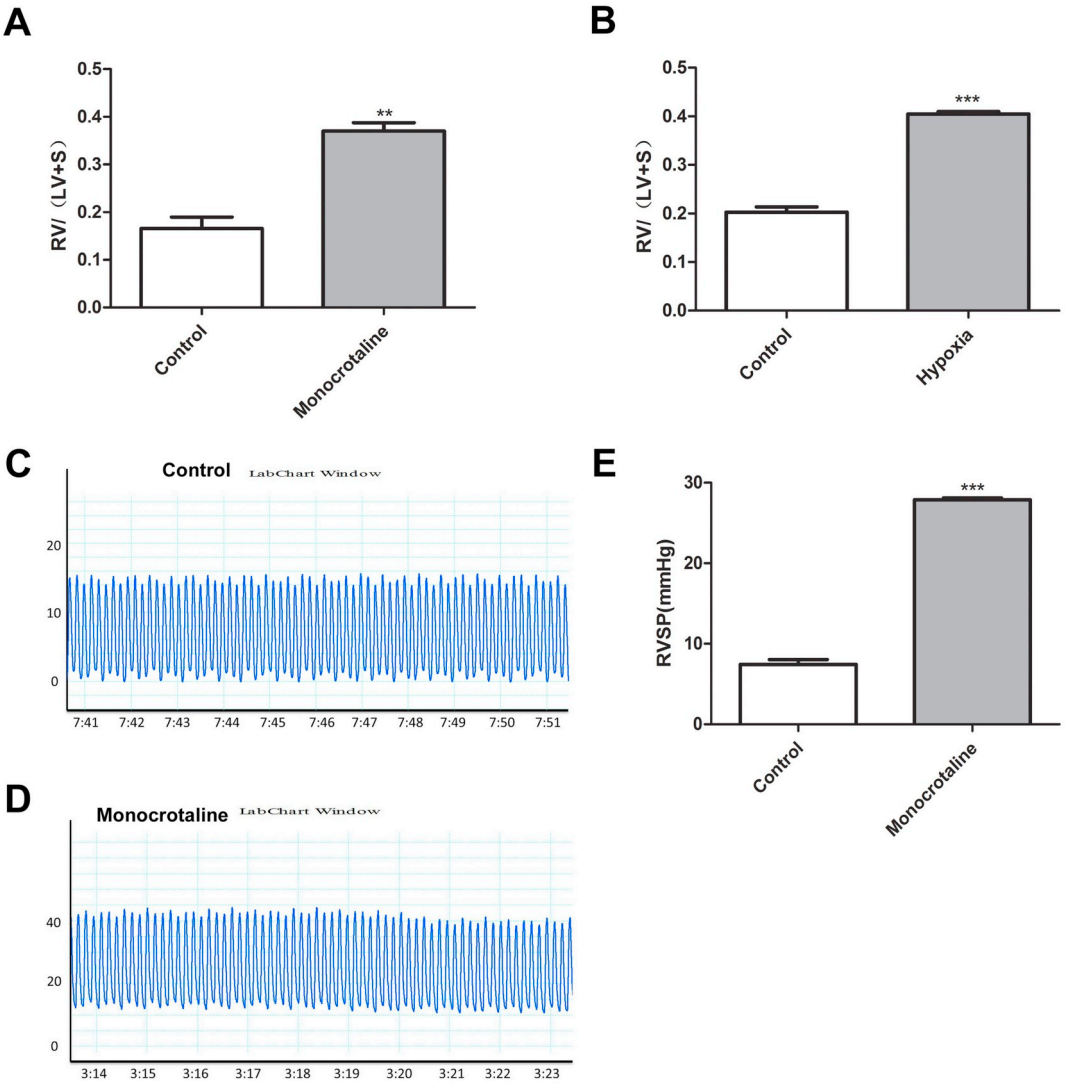

Fig. 1. RV hemodynamics and morphometry analysis in different group rats. (A): Changes in the right ventricle/ (left ventricle plus septum) (RV/LV + S) ratio in control group rats and monocrotaline group rats. (B) Changes in RV/LV + S ratio in control group rats and hypoxia rats. (C, D) Assessment of right ventricular systolic pressure in MCT-induced PAH rats and control rats. (E) Changes in right ventricular systolic pressure (RVSP). In control group rats and monocrotaline rats. Data are shown as means ± SD. Similar results were observed in three independent experiments. $^{**}P < .01$, $^{***}P < .001$.

thickness in the pulmonary artery. In addition, masson stain assay showed the photographs taken from different groups (Fig. 2E, G). There was a significant increase in the vascular collagen area of the pulmonary artery in hypoxia group rats and in monocrataline group rats (Fig. 2F, H). We used immunohistochemistry stain to determine the expression of α-SM-actin in the pulmonary artery vascular from rat lung tissues (Fig. 2I, J). The results showed the wall thickness of the pulmonary artery vascular was increased in hypoxia and monocrotaline groups. Meanwhile, the expression of α-SM-actin in the pulmonary artery vascular of two groups were increased compared with that of control group respectively. The results indicated that hypoxia and monocrotaline injection enhanced pulmonary artery vascular remodeling in the rats.

3.3. The expression of Stox1 protein was increased in lung tissues and pulmonary arterial vessels

To determine whether Stox1 was implicated in hypoxia-treated and monocrotaline injection induced pulmonary artery vascular remodeling, lung samples from hypoxia group rats and monocrotaline group rats were collected and assessed by immunohistochemistry stain. The results showed that thickened vessel walls were present in both hypoxia group rats (Fig. 3A) and the monocrotaline group rats (Fig. 3C), while the relative of vascular Stox1 expression of hypoxia group and monocrotaline group were over 2-time compared with that of control group respectively (Fig. 3B, D). To localize Stox1 expression in the lung vessels, Immunofluorescence of Stox1 protein was performed on pulmonary arterial vessels from different group rats. The results showed strong intensity staining of Stox1 in pulmonary artery in hypoxia group tissues and in monocrotaline group (Fig. 3E, F). The relative value of Stox1 expression in hypoxia group and monocrotaline group was significantly increased compared with that of control group by western blot assay (Fig. 3G, I). The increased value of Stox1 expression remained that Stox1 protein may play an important role in pulmonary artery vascular remodeling.

3.4. Stox1 expression was increased in hypoxia condition in vitro

Since the Stox1 protein was increased in lung tissues from hypoxia-treated rats, we endeavored to confirm whether Stox1 was involved in

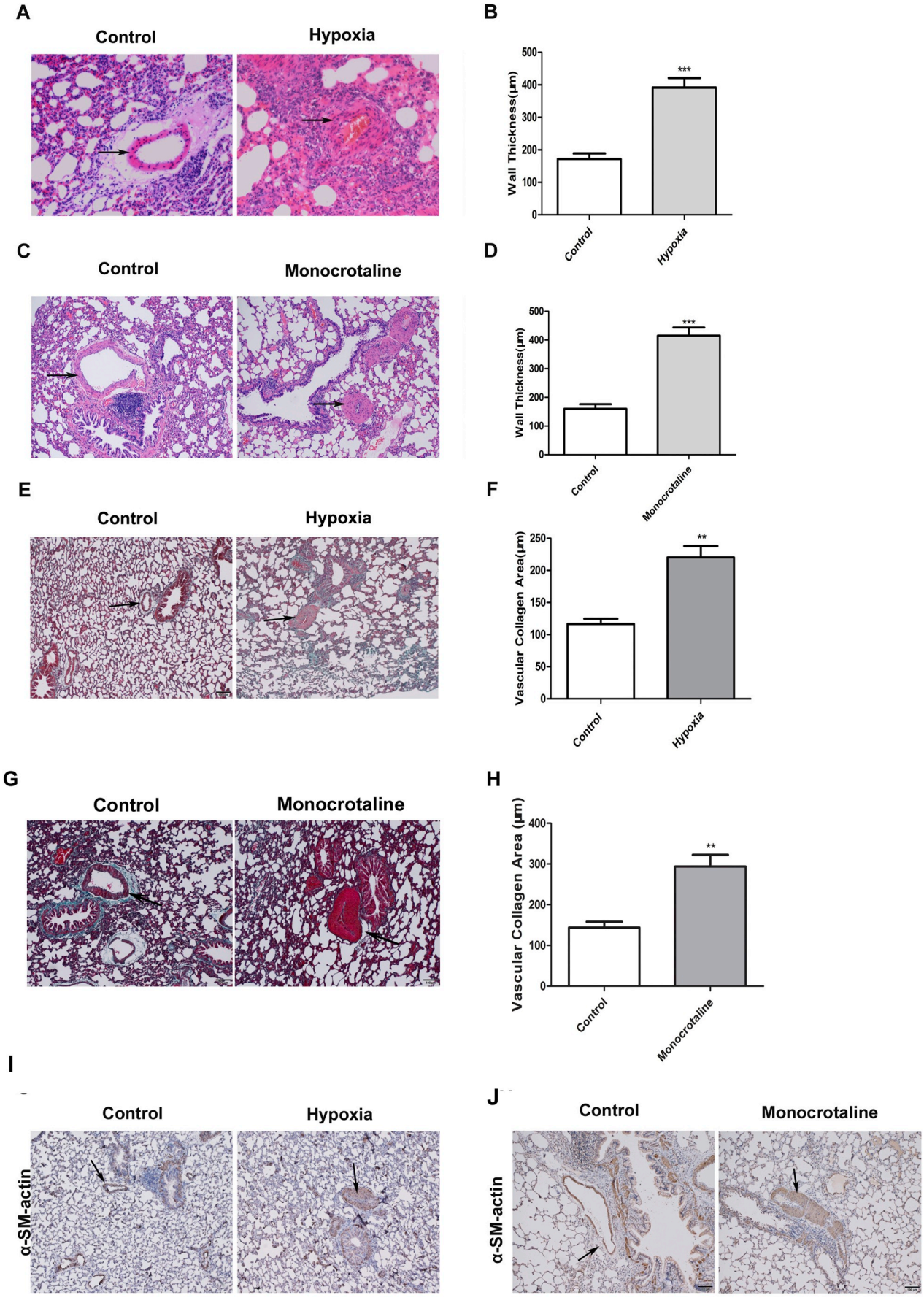

(caption on next page)

Fig. 2. Morphometric analysis of pulmonary vascular remodeling in lung tissues from the PAH rats. (A) HE staining showed pulmonary arterial vessels of lung tissues (magnification, x100).(B) Wall thickness of the pulmonary arterial vessels. (C) HE staining showed pulmonary arterial vessels of lung tissues (magnification, x100). (D) Wall thickness of the pulmonary arterial vessels. (E)Masson staining showed pulmonary arterial vessels of lung tissues (magnification, x100). (F) Vascular collagen area in the pulmonary arterial vessels. (G) Masson staining showed pulmonary arterial vessels of lung tissues (magnification, x100). (H) Vascular collagen area in the pulmonary arterial vessels. (I) Immunohistochemical evaluation of α-SM-actin expression in lung tissues(magnification, x100). (J) Immunohistochemical evaluation of α-SM-actin expression in lung tissues (magnification, x100). Data are shown as means ± SD. Similar results were observed in three independent experiments. $^{**}P < .01$, $^{***}P < .001$.

the proliferation of PASMCs. Next we explored the expression of Stox1 in PASMCs in hypoxia condition for 0 h, 12 h, 24 h and 48 h. As shown in Fig. 4A, the protein level of Stox1 was increased with time-dependent manner exposed to hypoxia (Fig. 4B). Moreover, we used the small infection solution to explore the effect of Stox1 on hypoxia-treated PASMCs. There were three solutions provided and the western blot assay was used to check effectiveness of inhibition of Stox1 protein (Fig. 4C). As shown in Fig. 4D, as the Stox1 expression in PASMCs was decreased after treated with small infection solutions, si-Stox1-rat-1194(si-3) solution was the most effective one for knockdown of Stox1 expression (Fig. 4D).

3.5. Proliferation and migration of hypoxia-induced PASMCs was inhibited by knocking down Stox1

Since pulmonary arterial vascular remodeling was induced by proliferation of PASMCs, we investigated whether Stox1 was influence on the regulation of PASMCs proliferation. We transfected PASMCs with si-3 solution and set the cells in hypoxia condition for 48 h. As shown in Fig. 5A, according to photograph by the EdU assay, the proliferation viability of PASMCs cultured in hypoxia condition was increased compared with the cells on normoxia condition used as control group, while the proliferation viability of PASMCs was decreased by transfected with si-3 compared with the cells in hypoxia group (Fig. 5B). Knockdown of Stox1 resulted in decreased in cell proliferation compared with that of hypoxia group, as measured by CCK-8 assay (Fig. 5C). To investigate the role of Stox1 in PASMCs migration, we used migration assay under microscope. As shown in Fig. 5D, hypoxia promoted PASMCs migration compared to the migration of control cells. Knockdown Stox1 induced a half decrease in the cell-covered area after 48 h (Fig. 5E). All the results mentioned above proved that Stox1 was taken part in the proliferation and migration on PASMCs, which reminded us to further explore the function of Stox1 on cell cycle in PASMCs.

3.6. Stox1 induced cell cycle arrest in PASMCs

Further study was focused on the cell cycle and the relative proteins expression. Cell cycle assays revealed a depression of S phase in siStox1-treated cells by flow cytometry (Fig. 6A, B) compared with that in hypoxia treated cells, which indicated Stox1 inhibited the cell cycle arrest induced by hypoxia in PASMCs. To investigate the molecular basis for this function of Stox1 in PASMCs, we measured levels of several cell cycle-related proteins including PCNA, Cyclin A and Cyclin E. PCNA performs critical functions during DNA replication in cell proliferation. Cyclin A preferentially stimulates microtubule-nucleating activity of centrosomes, and Cyclin E is a key regulator of G1-S transition. As shown in Fig. 6C, D, E, PCNA, Cyclin A and Cyclin E expression levels were significantly increased in hypoxia-treated PASMCs, while after treated with siStox1,the expression of proteins were reduced compared to hypoxia-treated samples (Fig. 6F, G, H).

3.7. Stox1 activated AKT signaling pathway in hypoxia PASMCs

We further examined whether AKT pathway was involved in the effect induced by Stox1 in PASMCs. As shown in Fig. 7A, hypoxia significantly increased phosphorylated AKT (p-AKT) protein level compared to that of control group. Then, we used RNA interference technology to knockdown the expression of Stox1. The results showed p-AKT expression was decreased compared to hypoxia group. In Fig. 7B, the ratio of the p-AKT to the total AKT was increased after hypoxia treated in PAMSCs while the ratio was decreased after knocking down Stox1 protein. These results indicated that AKT pathway may be involved in Stox1-induced functions of PASMCs under hypoxia.

4. Discussion

Based on the above data, we explored the expression property and biological function of the Stox1 protein in PAs and PASMCs. To the best of our knowledge, it is the first time to find that the Stox1 was expressed in PAs and PASMCs. We also demonstrated that Stox1 could both induce proliferation and cell cycle arrest in hypoxia-treated PASMCs. Meanwhile, at least in part, we detected that the Stox1 function on PASMCs was mediated via the AKT pathway. These results suggested that Stox1-AKT axis played an important role in pulmonary arterial vascular remodeling in response to hypoxia stress.

The STOX1, a transcription factor, was discovered in 2005, and winged helix DNA-binding domain showed great similarity to the binding domain seen in the family of FOX transcription factors. Also, its upstream regulation mechanism was also similar as seen in multiple members of the FOX transcription factor family, such as the PI3K-AKT pathway [23]. Studies have indicated that STOX1 appeared to have multiple gene targets, especially in pathways connected to inflammation, oxidative stress, and cell cycle [12]. Moreover, recently research shown that the gene was directly associated with genetic forms of preeclampsia (PE) [24]. Its overexpression in choriocarcinoma cells mimicked the transcriptional consequences of PE in the human placenta [25]. Further study showed that increased levels of IGF1 led to increased expression levels of STOX1 in extravillous trophoblasts via the MAPK pathway. Using inhibitors of the PI3K/AKT and MAPK pathway showed that the effect of IGF1 on STOX1 expression was accomplished via MAPK signaling [8]. Recently results showed that siSTOX1 inhibited phosphorylation of AKT in the inner ear utricular epithelial cells, while over-expression of STOX1 activated phosphorylation of AKT [10]. However, it is still unclear that the functional orientation, expression and the underling mechanisms of Stox1 activation on hypoxia-mediated proliferation in PAH.

This study demonstrated for the first time that Stox1 was over-expressed in the pulmonary vessels of PAH in hypoxia rats. Moreover, we discovered the Stox1 expression was up-regulated in time-dependent manner in vitro under hypoxia condition. To further validate the potential role of Stox1 in the development of PAH, we used siRNA to inhibit Stox1 expression in PASMCs. The proliferation of PASMCs was reflected indirectly by CCK-8 assay. The increased effect on cell viability of hypoxia-treated PASMCs was decreased after treated with siStox1 in PASMCs. Moreover, hypoxia induced the migration of PASMCs, which was inhibited by treated with siStox1 in PASMCs. As Stox1 affected the proliferation and migration of PASMCs, we further explored the function of the Stox1 on cell cycle progression. Eukaryotic cells replicate their chromosomes and partition them to two daughters, which is the cell division cycle process [26]. There are four phases in cell cycle, including G1 phase (before DNA replication), G2 phase

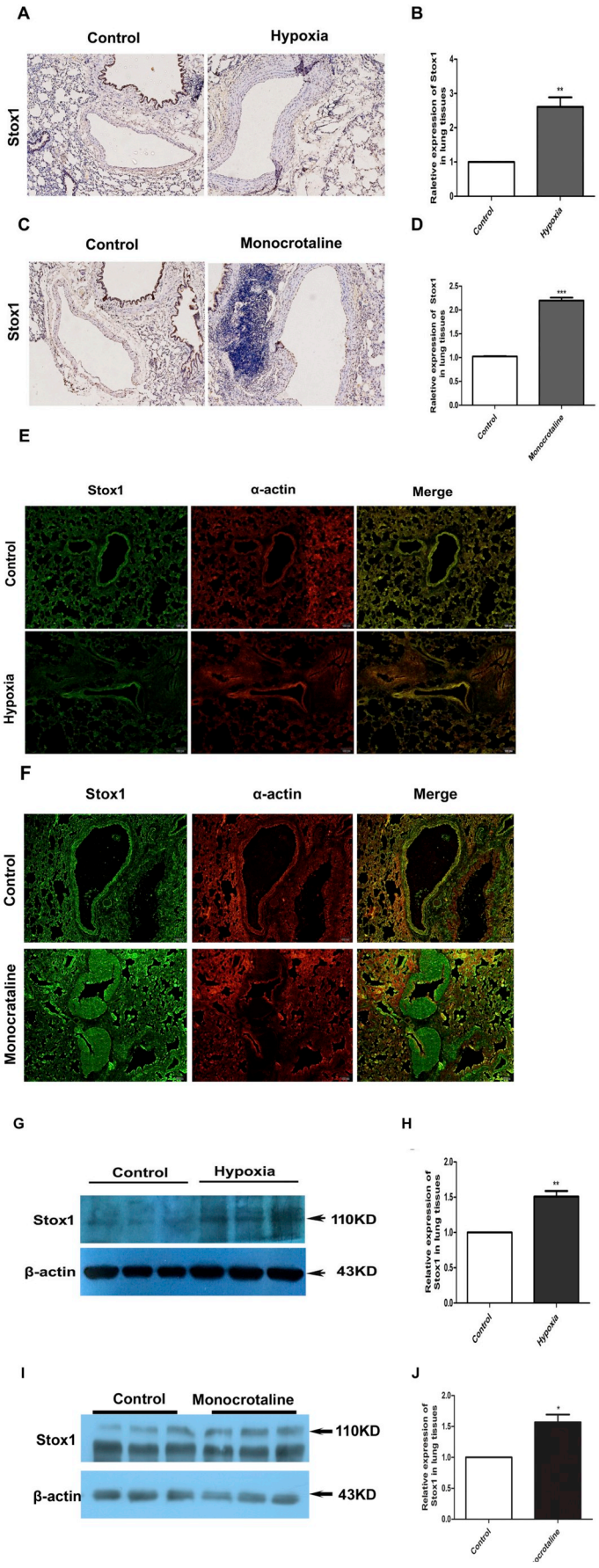

Fig. 3. Expression of Stox1 protein was increased in lung tissues and pulmonary arterial vessels in PAH rat model. (A) Immunohistochemical evaluation of Stox1 expression in lung tissues (magnification, x100). (B) Relative expression of Stox1 in lung tissues. (C) Immunohistochemical evaluation of Stox1 expression in lung tissues (magnification, x100). (D) Relative expression of Stox1 in lung tissues. (E) Immunofluorescence of Stox1 protein in pulmonary arterial vessels. (F) Immunofluorescence of Stox1 protein in pulmonary arterial vessels (magnification, x100). (G)The levels of Stox1 in lung tissues were measured by western blotting assay. (H) Densitometry was applied to quantify the protein density. (I) The levels of Stox1 in lung tissues were measured by western blotting assay. (J) Densitometry was applied to quantify the protein density. All of the values are denoted as the means ± SD. Data are representative of at least three independent experiments. $^{*}P < .05$, $^{**}P < .01$, $^{***}P < .001$.

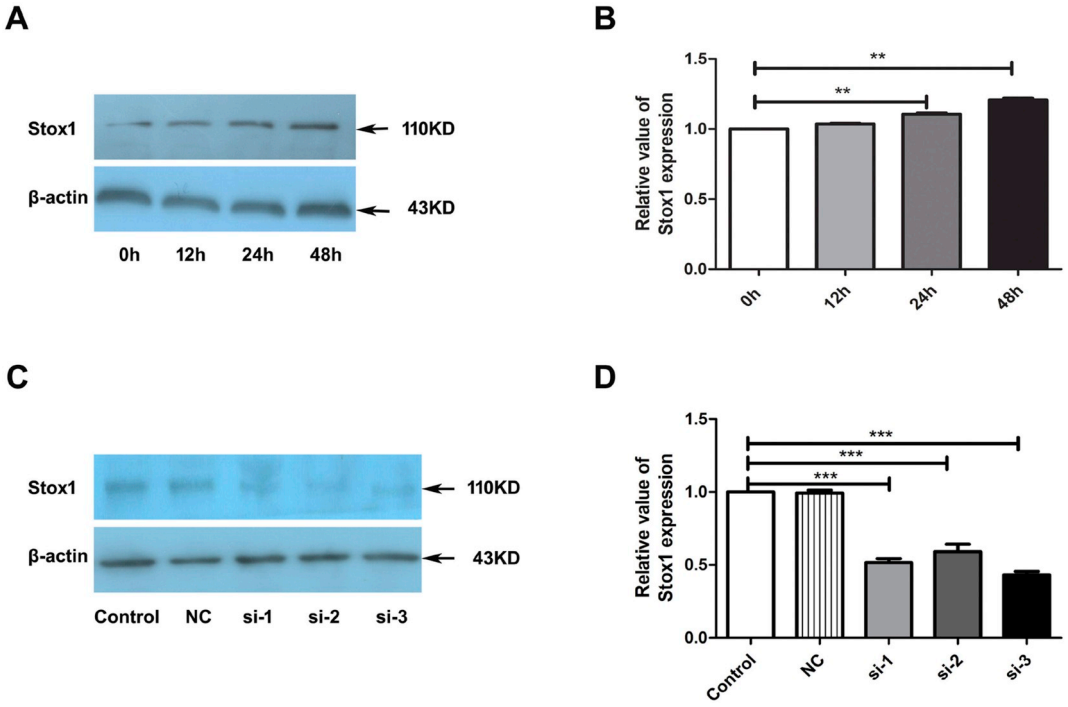

Fig. 4. Stox1 expressions were increased in hypoxia condition in vitro. (A)The expression of Stox1 was measured for 0 h, 12 h, 24 h and 48 h in PASMCs with hypoxia condition by western blot assay. (B) Relative expression of Stox1 in PASMCs. (C) Cells were treated with si-Stox1-rat-373, si-Stox1-rat-747, si-Stox1-rat-1194, negative control. Cells were treated with normoxia condition used as control group. Western blotting assay was used for checking the value of Stox1 protein expression. (D) Relative value of Stox1 expression in PASMCs. Data are shown as means ± SD. Similar results were observed in three independent experiments. Asterisk indicates significant difference as determined by one-way ANOVA. **P < .01, ***P < .001. NC means negative control, si-1 means si-Stox1-rat-373, si-2 means si-Stox1-rat-747, si-3 means si-Stox1-rat-1194.

(before mitosis), S phase (DNA replication) and M phase (chromosome segregation) [27]. The accurate transition from G1 phase of the cell cycle to S phase is crucial for the control of eukaryotic cell proliferation, and its out-of-order regulation promotes oncogenesis [28,29]. Our findings demonstrated that hypoxia enhanced the proportion of cells in the S phases, while the effect was inhibited after treated with siStox1, which suggested Stox1 may participant in cell cycle arrest in PASMCs. Meanwhile, to further confirm the function of Stox1 on cell cycle of PASMCs, we checked the expression of PCNA, Cyclin A and Cyclin E. PCNA was an essential substance in the DNA synthesis phase of eukaryotic cells and an important index for evaluating the status of cell proliferation [30]. The formation of the PCNA trimer is also essential for targeting the replication-licensing protein, chromatin-licensing, and DNA replication factor 1 (CDT1), for ubiquitin-dependent proteolysis to prevent chromosomal DNA re-replication [31]. Our results showed that blockade of the Stox1 with siStox1 decreased the expression of PCNA as the value of PCNA expression was increased in hypoxia-treated PASMCs. Cyclin A and Cyclin E were involved in the control of G2/M transition and mitosis. Our results showed that blockade of the Stox1 with siStox1 decreased the expression of Cyclin A and Cyclin E. As mentioned above, our results indicated that Stox1 was mediated the hypoxia-induced cell proliferation, migration and cell cycle progression in PASMCs.

During mammalian organogenesis, the AKT pathway promotes both cell proliferation and programmed cell death in hypoxia-induced PAH [32]. Bioinformatics analysis was used to identify AKT signaling pathway. As stated previously, hypoxia induced and promoted the expression of AKT signaling pathway and the radio of phosphorylation to total protein levels of AKT were abolished by knockdown of Stox1 in PASMCs. Accumulating evidence has indicated that the activation of AKT pathway contributed to pulmonary vascular medial thicken, migration, proliferation and cell cycle arrest of PASMCs [33].

In addition, the cell viability and migration was increased by time-dependent manner under hypoxia exposure but reversed by blocking Stox1 with small molecule interference in PASMCs. Meanwhile, we indicated cell cycle progression and relative proteins expression, including PCNA, Cyclin A and Cyclin E. The percentage of cells in the S phase was enhanced and the expression of relative proteins was increased in hypoxia condition, while all the results were decreased by administration of siStox1. Furthermore, hypoxia significantly enhanced the ratio of phosphorylation to total protein expression of AKT, while the effects were reduced after treated with siStox1 in PASMCs. This phenomenon argued that the activation of AKT was involved in the Stox1 effect on proliferation, migration, cell cycle and signaling pathway.

However, there remained further investigation for us to explore the function of Stox1 in PASMCs. Firstly, the expression of Stox1 was identified only in PAH rat models and further study should focus on validation in patients with PH [34]. Secondly, as AKT was a downstream target of PI3K pathway, it is also important in revealing the relationship of Stox1 and PI3K/AKT pathway [35]. Moreover, it is not clear that the complexes interaction between the PI3K/AKT signaling pathway and regulation of transcription and translation level of Stox1 in PASMCs, which should be addressed in future studies.

5. Conclusions

In conclusion, we revealed the expression of Stox1 in pulmonary artery vessels in PAH and determined the role of Stox1 in proliferation and migration of PASMCs. Our current results showed that Stox1

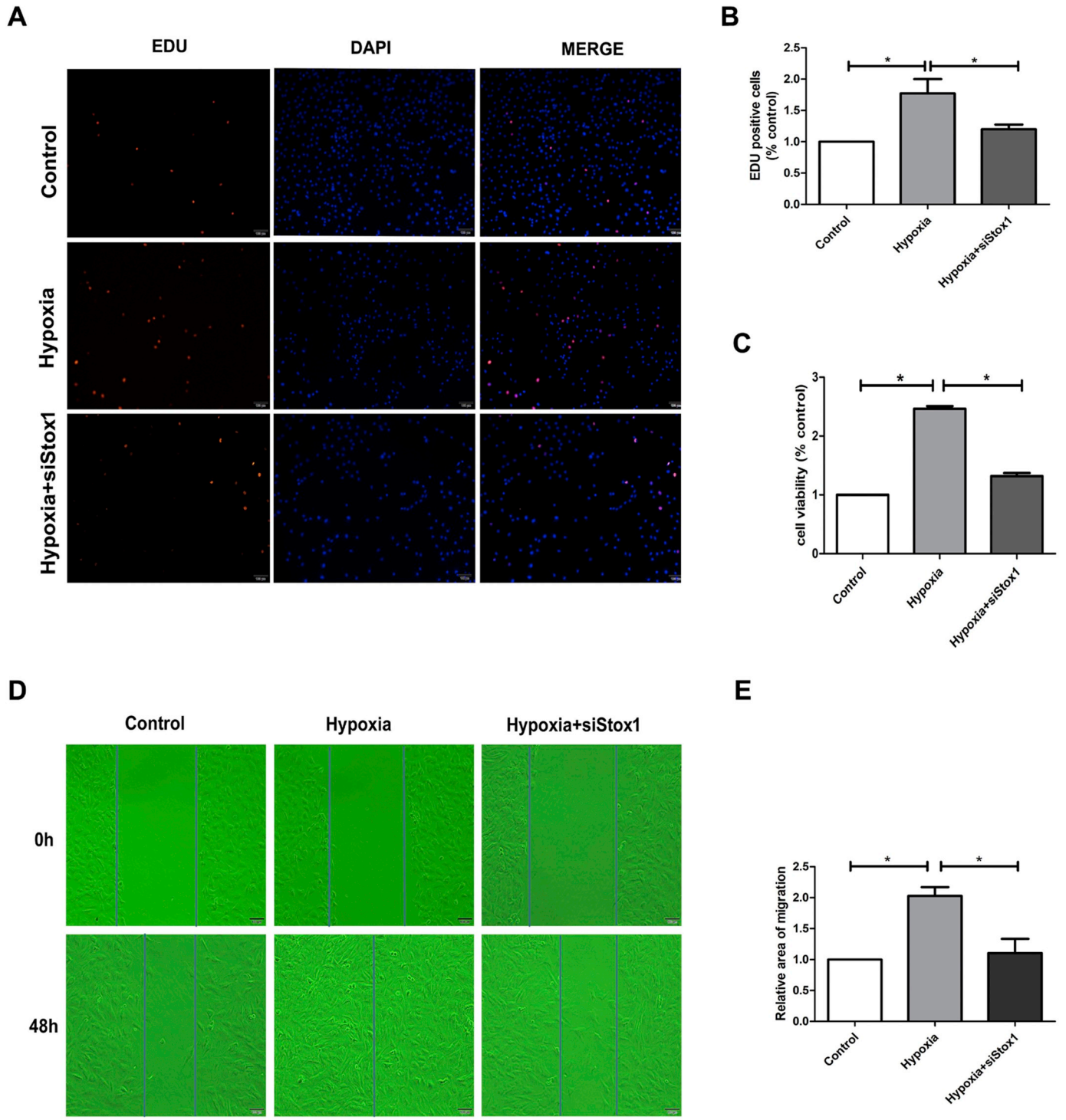

Fig. 5. Proliferation and migration of hypoxia-induced PASMCs was inhibited by knocking down Stox1. (A) Fluorescence images of PASMCs were shown by 5-Ethynyl-2′-deoxyuridine (EdU) staining. The cells were cultured with normoxia condition, hypoxia condition, and hypoxia condition with infection siStox1. (B) Proliferation viability of cells was analysis according to fluorescence images. (C) CCK-8 assay was used for cell viability in PASMCs. (D) Cell migration pictures of PASMCs were taken at different conditions representatively. (E) Relative area of migration of PASMCs in different condition was shown in histogram. Data are shown as means ± SD. Similar results were observed in three independent experiments. Asterisk indicates significant difference as determined by one-way ANOVA. $^{*}P < .05$.

inhibition and silencing decreased the effect of proliferation, migration and cell cycle arrest induced by hypoxia in PASMCs. Furthermore, we elucidated that the AKT pathway mediated, at least in part, the role of Stox1 in hypoxia pulmonary vascular remodeling, which included the effect on cell viability, cell cycle progression in PASMCs. Stox1 played an important role in the pulmonary vascular remodeling in PAH through AKT signaling. Because vascular remodeling is now recognized as a major prognostic marker in patients at PAH, Stox1 may represent an interesting pharmacological target greatly helpful in the development of new therapeutic strategies for PAH.

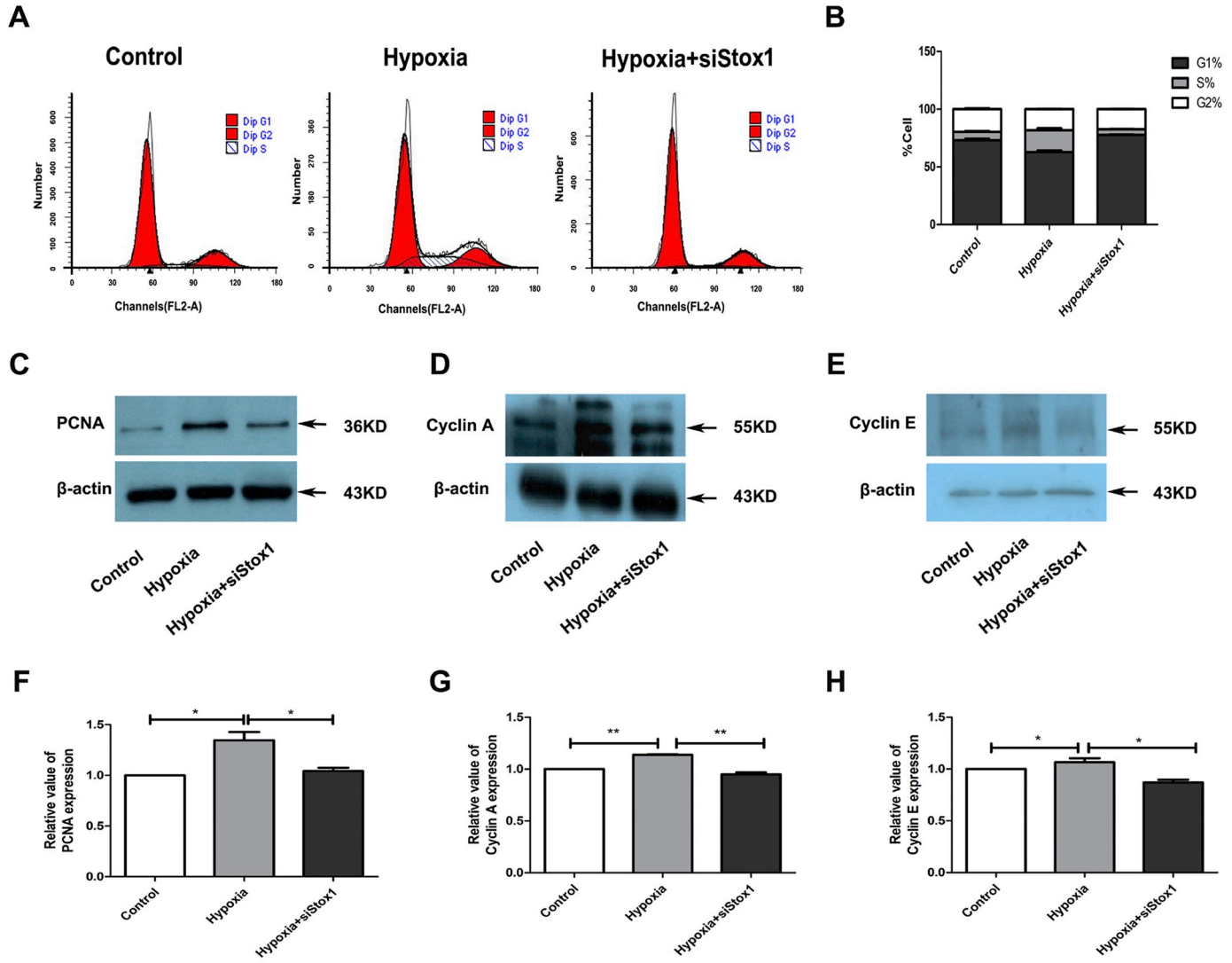

Fig. 6. Stox1 induced cell cycle arrest in PASMCs. (A) Flow cytometry plots. (B) Quantitative analysis of flow cytometry results on cell cycle progression. (C, D, E) Protein levels of PCNA, Cyclin E, Cyclin A were analyzed by western-blotting. (F, G, H) Densitometry quantification of proteins bands was shown after 48 h transfection with siStox1. Data are shown as means ± SD. Similar results were observed in three independent experiments. Asterisk indicates significant difference as determined by one-way ANOVA. $*P < .05$, $**P < .01$.

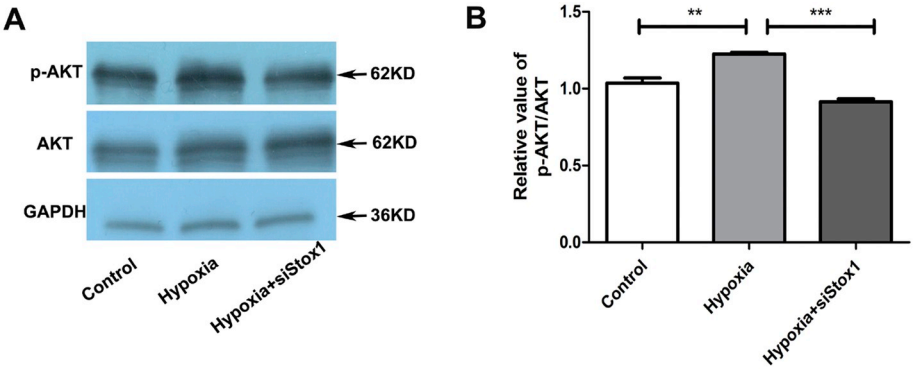

Fig. 7. Expression of p-AKT and total AKT in PASMCs in hypoxia and hypoxia with siStox1. (A) Protein levels of p-AKT and total AKT were determined by western blotting. (B) Densitometry quantification of proteins bands was shown. Data are shown as means ± SD. Similar results were observed in three independent experiments. Asterisk indicates significant difference as determined by one-way ANOVA. $**P < .01$, $***P < .001$.

Funding information

This work was supported by grants from National Natural Science Foundation of China (31871155), grants from the Natural Science Foundation of Jiangsu Province (BK20161297), grants from National Science Foundation of China (31871155), the Social Fund for Development of Lianyungang Science and Technology Bureau (SH1612), project of Jiangsu Provincial Commission of Health and Family Planning (QNRC2016505), Six big talent peak C projects (YY-110),the Young Talent Project of the First People's Hospital of Lianyungang (1701).

Declaration of Competing Interest

The authors declare no conflict of interest.

References

[1] N.C. Bacha, M. Levy, C.L. Guerin, B. Le Bonniec, A. Harroche, I. Szezepanski, J.M. Renard, P. Gaussem, D. Israel-Biet, C.M. Boulanger, D.M. Smadja, Treprostinil treatment decreases circulating platelet microvesicles and their procoagulant activity in pediatric pulmonary hypertension, Pediatr. Pulmonol. 54 (1) (2019) 66–72, https://doi.org/10.1002/ppul.24190.

[2] C.Y. Zhang, M. Liu, J.M. Wan, M.Q. Gao, Y. Zhang, M. Soyan, H.L. Wang, Y. Bai, Role of noncoding RNA in pulmonary arterial hypertension and potential drug therapeutic target, Curr. Top. Med. Chem. 18 (12) (2018) 975–986.

[3] Z. Zhang, H. Sun, H. Dai, R.M. Walsh, M. Imakura, J. Schelter, J. Burchard, X. Dai, A.N. Chang, R.L. Diaz, J.R. Marszalek, S.R. Bartz, M. Carleton, M.A. Cleary, P.S. Linsley, C. Grandori, MicroRNA miR-210 modulates cellular response to hypoxia through the MYC antagonist MNT, Cell Cycle (Georgetown, Tex.) 8 (17) (2009) 2756–2768.

[4] Y. Sun, X. Lin, L. Li, Identification of biomarkers for Schistosoma-associated pulmonary arterial hypertension based on RNA-Seq data of mouse whole lung tissues, Lung 195 (3) (2017) 377–385.

[5] L. Zhang, Y.M. Li, X.X. Zeng, X.Y. Wang, S.K. Chen, L.X. Gui, M.J. Lin, Galectin-3-mediated transdifferentiation of pulmonary artery endothelial cells contributes to hypoxic pulmonary vascular remodeling, Cell. Physiol. Biochem. 51 (2) (2018) 763–777, https://doi.org/10.1159/000495331.

[6] M.H. Fenstad, M.P. Johnson, M. Loset, S.B. Mundal, L.T. Roten, I.P. Eide, L. Bjorge, R.K. Sande, A.K. Johansson, T.D. Dyer, S. Forsmo, J. Blangero, E.K. Moses, R. Austgulen, STOX2 but not STOX1 is differentially expressed in decidua from pre-eclamptic women: data from the second nord-trondelag health study, Mol. Hum. Reprod. 16 (12) (2010) 960–968.

[7] V. Rigourd, C. Chauvet, S.T. Chelbi, R. Rebourcet, F. Mondon, F. Letourneur, T.M. Mignot, S. Barbaux, D. Vaiman, STOX1 overexpression in choriocarcinoma cells mimics transcriptional alterations observed in preeclamptic placentas, PLoS One 3 (12) (2008) e3905.

[8] H.K. Thulluru, C. Park, D. Dufort, G. Kleiverda, C. Oudejans, M. van Dijk, Maternal NODAL inversely affects NODAL and STOX1 expression in the fetal placenta, Front. Genet. 4 (2013) 170, , https://doi.org/10.3389/fgene.2013.00170.

[9] L. Doridot, L. Chatre, A. Ducat, J.L. Vilotte, A. Lombes, C. Mehats, S. Barbaux, R. Calicchio, M. Ricchetti, D. Vaiman, Nitroso-redox balance and mitochondrial homeostasis are regulated by STOX1, a pre-eclampsia-associated gene, Antioxid. Redox Signal. 21 (6) (2014) 819–834, https://doi.org/10.1089/ars.2013.5661.

[10] X. Nie, K. Zhang, L. Wang, G. Ou, H. Zhu, W.Q. Gao, Transcription factor STOX1 regulates proliferation of inner ear epithelial cells via the AKT pathway, Cell Prolif. 48 (2) (2015) 209–220.

[11] D. Vaiman, F. Miralles, Targeting STOX1 in the therapy of preeclampsia, Expert Opin. Ther. Targets 20 (12) (2016) 1433–1443.

[12] C. Zhang, Z. Ji, W. Zhang, R. Yang, H. An, R. Yang, D. van Abel, M. van Dijk, X. Yang, G. Ou, H.H. Zhu, W.Q. Gao, Stox1 as a novel transcriptional suppressor of Math1 during cerebellar granule neurogenesis and medulloblastoma formation, Cell Death Differ. 23 (12) (2016) 2042–2053, https://doi.org/10.1038/cdd.2016.85.

[13] D. van Abel, O. Abdulhamid, W. Scheper, M. van Dijk, C.B. Oudejans, STOX1A induces phosphorylation of tau proteins at epitopes hyperphosphorylated in Alzheimer's disease, Neurosci. Lett. 528 (2) (2012) 104–109.

[14] D. van Abel, O. Michel, R. Veerhuis, M. Jacobs, M. van Dijk, C.B. Oudejans, Direct downregulation of CNTNAP2 by STOX1A is associated with Alzheimer's disease, J. Alzheimer's Dis.: JAD 31 (4) (2012) 793–800.

[15] Y. Liu, Z. Sun, J. Zhu, B. Xiao, J. Dong, X. Li, LncRNA-TCONS_00034812 in cell proliferation and apoptosis of pulmonary artery smooth muscle cells and its mechanism, J. Cell. Physiol. 233 (6) (2018) 4801–4814.

[16] Z. Xiaoji, M. Xiao, X. Rui, C. Haibo, Z. Chao, L. Chengjin, W. Tao, G. Wenjun, Z. Shengming, Mechanism underlying acute lung injury due to sulfur mustard exposure in rats, Toxicol. Ind. Health 32 (8) (2016) 1345–1357.

[17] W.X. Xin, Q.L. Li, L. Fang, L.K. Zhong, X.W. Zheng, P. Huang, Preventive effect and mechanism of ethyl acetate extract of sceptridium ternatum in monocrotaline-induced pulmonary arterial hypertension, Chinese J. Integr. Med. (2018).

[18] D. Karpuz, O. Hallioglu, B. Buyukakilli, S. Gurgul, E. Balli, M. Ozeren, B. Tasdelen, Clinical and histopathological relationship of sildenafil and bosentan treatments in rats with monocrotaline induced pulmonary hypertension, Bratisl. Lek. Listy 118 (9) (2017) 544–551.

[19] Y. Li, W. Ren, X. Wang, X. Yu, L. Cui, X. Li, X. Zhang, B. Shi, MicroRNA-150 relieves vascular remodeling and fibrosis in hypoxia-induced pulmonary hypertension, Biomed. Pharmacother. 109 (2019) 1740–1749, https://doi.org/10.1016/j.biopha.2018.11.058.

[20] Y. Fan, J. Zhao, J. Qian, Y. Hao, W. Qian, L. Gao, M. Li, X. Zeng, Z. Zhang, Cysteine-rich protein 61 as a novel biomarker in systemic lupus erythematosus-associated pulmonary arterial hypertension, Clin. Exp. Rheumatol. (2018).

[21] L.N. Wang, W.C. Yu, C.H. Du, L. Tong, Z.Z. Cheng, Hypoxia is involved in hypoxic pulmonary hypertension through inhibiting the activation of FGF2 by miR-203, Eur. Rev. Med. Pharmacol. Sci. 22 (24) (2018) 8866–8876.

[22] L. Zhang, C. Ma, R. Gu, M. Zhang, X. Wang, L. Yang, Y. Liu, Y. Zhou, S. He, D. Zhu, Paeonol regulates hypoxia-induced proliferation of pulmonary artery smooth muscle cells via EKR 1/2 signalling, Eur. J. Pharmacol. 834 (2018) 257–265.

[23] M. van Dijk, C.B. Oudejans, STOX1: key player in trophoblast dysfunction underlying early onset preeclampsia with growth retardation, J. Pregnancy (2011) (2011) 521826.

[24] H.K. Thulluru, C. Park, D. Dufort, G. Kleiverda, C. Oudejans, M. van Dijk, Maternal NODAL inversely affects NODAL and STOX1 expression in the fetal placenta, Front. Genet. 4 (2013) 170.

[25] L. Doridot, B. Passet, C. Mehats, V. Rigourd, S. Barbaux, A. Ducat, F. Mondon, M. Vilotte, J. Castille, M. Breuiller-Fouche, N. Daniel, F. le Provost, A.L. Bauchet, V. Baudrie, A. Hertig, C. Buffat, U. Simeoni, G. Germain, J.L. Vilotte, D. Vaiman, Preeclampsia-like symptoms induced in mice by fetoplacental expression of STOX1 are reversed by aspirin treatment, Hypertension 61 (3) (2013) 662–668.

[26] M. Hopkins, J.J. Tyson, B. Novak, Cell-cycle transitions: a common role for stoichiometric inhibitors, Mol. Biol. Cell 28 (23) (2017) 3437–3446.

[27] J. Boehme, X. Sun, K.V. Tormos, W. Gong, M. Kellner, S.A. Datar, R.J. Kameny, J.X. Yuan, G.W. Raff, J.R. Fineman, S.M. Black, E. Maltepe, Pulmonary artery smooth muscle cell hyperproliferation and metabolic shift triggered by pulmonary overcirculation, Am. J. Physiol. Heart Circ. Physiol. 311 (4) (2016) H944–h957.

[28] C. Bertoli, J.M. Skotheim, R.A. de Bruin, Control of cell cycle transcription during G1 and S phases, Nat. Rev. Mol. Cell Biol. 14 (8) (2013) 518–528.

[29] J.P. Matson, J.G. Cook, Cell cycle proliferation decisions: the impact of single cell analyses, FEBS J. 284 (3) (2017) 362–375.

[30] C.G. Havens, J.C. Walter, Docking of a specialized PIP box onto chromatin-bound PCNA creates a degron for the ubiquitin ligase CRL4Cdt2, Mol. Cell 35 (1) (2009) 93–104, https://doi.org/10.1016/j.molcel.2009.05.012.

[31] F. Leng, L. Saxena, N. Hoang, C. Zhang, Proliferating cell nuclear antigen interacts with the CRL4 ubiquitin ligase subunit CDT2 in DNA synthesis-induced degradation of CDT1, J. Biol. Chem. 293 (49) (2018) 18879–18889, https://doi.org/10.1074/jbc.RA118.003049.

[32] H. Tang, W. Lv, W. Sun, Q. Bi, Y. Hao, miR505 inhibits cell growth and EMT by targeting MAP3K3 through the AKTNFkappaB pathway in NSCLC cells, Int. J. Mol. Med. 43 (3) (2018) 1203–1216.

[33] Y. Xiao, H. Peng, C. Hong, Z. Chen, X. Deng, A. Wang, F. Yang, L. Yang, C. Chen, X. Qin, PDGF promotes the Warburg effect in pulmonary arterial smooth muscle cells via activation of the PI3K/AKT/mTOR/HIF-1alpha signaling pathway, Cell. Physiol. Biochem. 42 (4) (2017) 1603–1613, https://doi.org/10.1159/000479401.

[34] H. Collinot, C. Marchiol, I. Lagoutte, F. Lager, N. Siauve, G. Autret, D. Balvay, G. Renault, L.J. Salomon, D. Vaiman, Preeclampsia induced by STOX1 overexpression in mice induces intrauterine growth restriction, abnormal ultrasonography and BOLD MRI signatures, J. Hypertens. 36 (6) (2018) 1399–1406.

[35] Z. Li, G. Zhou, L. Jiang, H. Xiang, Y. Cao, Effect of STOX1 on recurrent spontaneous abortion by regulating trophoblast cell proliferation and migration via the PI3K/AKT signaling pathway, J. Cell. Biochem. (2018), https://doi.org/10.1002/jcb.28112.